Hyperbolization of Higher-Order PDEs: Theory, Applications, and Numerical Methods

Abhijit Biswas

Innovative and Efficient Strategies for Stiff Differential Equations at ICERM, Brown University, USA

July 23, 2025

Joint work with: D. Ketcheson, H. Ranocha, J. Schütz, C. Muñoz, L. Busaleh, M. Rajvanshi

ODEs as first-order systems

$$u''(t) + u(t)u'(t) = 0$$

With $u = q_0, \quad u'(t) = q_1$

$$\begin{cases} q_0'(t) &= q_1(t), \\ q_1'(t) &= -q_0(t)q_1(t). \end{cases}$$

- We can solve all ODEs with numerical methods designed for first-order systems
- If we understand first-order systems, we understand all ODEs

Hyperbolization: Hyperbolization allows us to do the same, but approximately, for time-evolutionary PDEs!

Hyperbolization of the heat equation

- $\partial_t u = \partial_x^2 u$, with $v(x,t) = \partial_x u$: $\begin{cases} \partial_t u & = \partial_x v \\ \partial_x u & = v. \end{cases}$
- Time evolutionary system: $\begin{cases} \partial_t u & = \partial_x v \\ \tau \partial_t v & = (\partial_x u - v), \end{cases}$ with $\tau > 0$.
- With $q = [u, v]^T$, the system can be written in the form

$$\partial_t q + A \partial_x q = Bq \;, \tag{1}$$

where $A = \begin{bmatrix} 0 & -1 \\ -\tau^{-1} & 0 \end{bmatrix}$ and $B = \begin{bmatrix} 0 & 0 \\ 0 & -\tau^{-1} \end{bmatrix}$.

Hyperbolicity and linear dispersion relation

Hyperbolicity: With $\tau > 0$, the matrix $A = \begin{bmatrix} 0 & -1 \\ -\tau^{-1} & 0 \end{bmatrix}$ is diagonalizable with eigenvalues $\pm\sqrt{\tau^{-1}}$, so this system is hyperbolic.

Dispersion relation: Solution ansatz: $q(x,t) = \mathbf{c}\exp(i(kx - \omega t))$

$$\omega_{\pm}(k) = \frac{i}{2\tau}\left(-1 \pm \sqrt{1 - 4k^2\tau}\right) \quad (2)$$

$$= \frac{i}{2\tau}\left(-1 \pm \left(1 - 2k^2\tau\right)\right) + \mathcal{O}(k^4\tau). \quad (3)$$

- $\omega_+(k) \approx -ik^2$, so the dispersion relation is approximately preserved.
- $\omega_-(k)$: spurious mode decays as $\tau \to 0$.

Numerical approximation

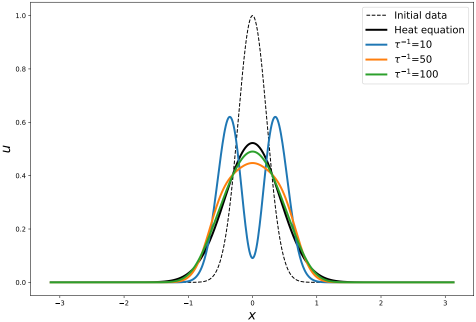

The parameter $\tau > 0$; as $\tau \to 0$, the solution of the hyperbolized heat equation tends to that of the heat equation.

Other examples

- Heat equation (Cattaneo 1958, Vernotte 1958)
- More general 2nd/3rd-order PDEs (Toro & Montecinos 2014, Mazaheri et. al. 2016)
- Defocusing NLS (Dhaouadi, Favrie & Gavrilyuk 2019)
- Conduit equation (Gavrilyuk, Nkongo & Shyue 2024)
- Dispersive shallow water (Antuouno et. al. 2009, Grosso et. al. 2010)
- Serre-Green-Naghdi (Favrie & Gavrilyuk 2017; Bassi et. al. 2020)
- Sainte-Marie (Escalante, Dumbser, & Castro 2019)
- Shear shallow water (Chesnokov & Nguyen 2019)
- Benjamin-Bona-Mahoney (Gavrilyuk & Shyue 2022)
- Korteweg-de Vries (Besse et. al. 2022)

Motivation

- (Potentially) efficient numerical solution: eliminate stiffness from high-order spatial derivatives

$$\partial_t u = \partial_{xx} u$$
$$\Delta t \propto \Delta x^2$$

$$\begin{cases} \partial_t u = \partial_x v \\ \tau \partial_t v = (\partial_x u - v) \end{cases}$$
$$\Delta t \propto \sqrt{\tau} \Delta x$$

- (Potentially) easier imposition of numerical boundary conditions
- Hyperbolization is likely more beneficial in higher dimensions, with non-periodic boundaries
- If "enough" accuracy can be achieved with a relatively large value of τ
- Well-developed theory and numerical methods
- Mathematical elegance: reduce all PDEs to a unified form

Existing hyperbolization approaches

- Cattaneo's relaxation approach
- Jin-Xin relaxation approach
- Extended Lagrangian approach

No general prescription for higher-order PDEs!

Systematic hyperbolization approach: Linearized KdV

$$\partial_t u + \partial_x^3 u = 0.$$

- Introduce new variables $q_0 \approx u$, $q_1 \approx \partial_x u$, and $q_2 \approx \partial_x^2 u$.
- Possible first order systems with $\tau > 0$:

$$\begin{cases} \partial_t q_0 + \partial_x q_2 = 0 \\ \tau \partial_t q_1 = \pm(q_1 - \partial_x q_0) \\ \tau \partial_t q_2 = \pm(q_2 - \partial_x q_1) \end{cases} \qquad \begin{cases} \partial_t q_0 + \partial_x q_2 = 0 \\ \tau \partial_t q_1 = \pm(q_2 - \partial_x q_1) \\ \tau \partial_t q_2 = \pm(q_1 - \partial_x q_0) \end{cases}$$

- Each of these systems is of the form $Dq_t + Aq_x = Bq$.
- There are eight possible hyperbolizations — how do we choose the best one?

The unique stable hyperbolization

- For a stable hyperbolic approximation, $\text{Im}(\omega) \leq 0$ must hold for the solution ansatz $q(x,t) = \mathbf{c}e^{i(kx-\omega t)}$
- The linear dispersion relation satisfies a cubic polynomial in ω for each system
- The linearized KdV equation admits a unique stable hyperbolization:

$$\begin{cases} \partial_t q_0 + \partial_x q_2 = 0 \\ \tau \partial_t q_1 = -(q_2 - \partial_x q_1) \\ \tau \partial_t q_2 = (q_1 - \partial_x q_0) \end{cases}$$

Hyperbolic approximation of KdV

$$\partial_t u + u\partial_x u + \partial_x^3 u = 0. \tag{4}$$

- New variables $q_0 \approx u$, $q_1 \approx \partial_x u$, and $q_2 \approx \partial_x^2 u$.
- The unique stable hyperbolization of the KdV equation:

$$\begin{cases} \partial_t q_0 + q_0\partial_x q_0 + \partial_x q_2 = 0 \\ \tau\partial_t q_1 = -(q_2 - \partial_x q_1) \\ \tau\partial_t q_2 = (q_1 - \partial_x q_0) \end{cases} \tag{5}$$

We require $\tau > 0$ and we expect that the solution of (5) approaches that of (4) as $\tau \to 0$.

Hyperbolic approximation of KdV

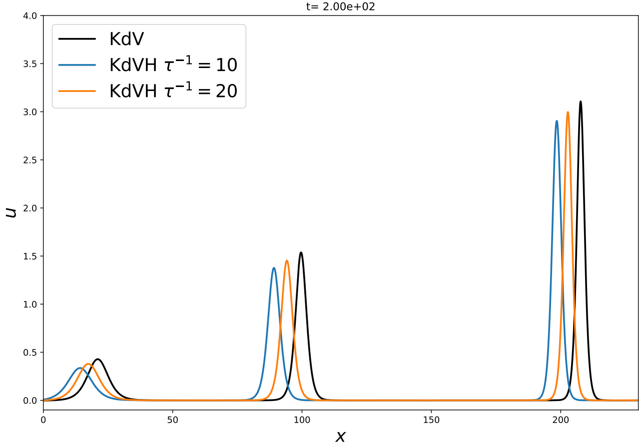

Figure: Comparison of the solution of the KdV equation (4) and its hyperbolic approximation (5). The approximation improves with smaller values of τ.

Hyperbolization of high-order PDEs

- Can this be done for general PDEs?
- Can it be done in a stable manner?
- How should one choose the structure (signs, ordering of relaxation terms) of the hyperbolic system?

Hyperbolization of a linear model equation

The linear model equation

$$\partial_t u + \sigma_0 \partial_x^m u = 0 \tag{6a}$$

$$u(x,0) = u_0(x) \tag{6b}$$

$$\text{where } \sigma_0 = \begin{cases} \pm 1 & m \text{ odd} \\ (-1)^{m/2} & m \text{ even.} \end{cases} \tag{6c}$$

- Introduce new variables $q_j \approx \partial_x^j u$ for $j = 0, 1, 2, \ldots, m-1$.
- Possible first order systems:

$$\partial_t q_0 + \sigma_0 \partial_x q_{m-1} = 0 \tag{7a}$$

$$\tau \partial_t q_j = \sigma_j (q_{i_j} - \partial_x q_{i_j - 1}) \quad j = 1, 2, \ldots, m-1, \tag{7b}$$

where $\tau > 0$, $\sigma_j = \pm 1$, and $\{i_1, i_2, \ldots, i_{m-1}\}$ is a permutation of the integers from 1 to $m-1$.

Structure of the hyperbolic system

- Write (7) in matrix form as

$$D\partial_t q + A\partial_x q = Bq. \tag{8a}$$

where

$$A = \begin{bmatrix} 0 & \sigma_0 \\ P & 0 \end{bmatrix} \quad B = \begin{bmatrix} 0 & 0 \\ 0 & P \end{bmatrix}, \quad D = \begin{bmatrix} 1 & & & \\ & \tau & & \\ & & \ddots & \\ & & & \tau \end{bmatrix}, \tag{8b}$$

and P is a signed permutation matrix of size $m-1$.

- Apply the ansatz $q(x,t) = \mathbf{c}\exp(i(kx-\omega t))$ and find the dispersion relation given by the solution of

$$\det(-i\omega D + ikA - B) = 0. \tag{9}$$

- The solution is stable only if $\mathrm{Im}(\omega)$ is non-positive.

Necessary conditions for stability

- Enough to study the case with $\tau = 1$
- **Low-wavenumber stability:**
  - With $k = 0$: $\det(\omega I - iB) = 0$.
  - Stability requires the eigenvalues of B must be in closed left half-plane
- **High-wavenumber stability:**
  - The high-wavenumber limiting dispersion relation: $\det(c(k)I - A) = 0$, where $c(k) = \omega(k)/k$.
  - The equation $\det(c(k)I - A) = 0$ is the dispersion relation of first order system $q_t + Aq_x = 0$.
  - The solution of this system is stable if and only if A has only real eigenvalues.

Unique hyperbolization

$$\partial_t u + \sigma_0 \partial_x^m u = 0 \quad \xrightarrow{\text{hyperbolization}} \quad D\partial_t q + A\partial_x q = Bq \ ,$$

where $A = \begin{bmatrix} 0 & \sigma_0 \\ P & 0 \end{bmatrix}$ and $B = \begin{bmatrix} 0 & 0 \\ 0 & P \end{bmatrix}$.

- The necessary conditions for stability of low- and high-wavenumbers uniqly determine the matrices A and B via choosing the permutation matrix $P = (p_{ij})$ given by

$$p_{ij} = \begin{cases} 0 & i+j \neq m \\ \sigma_0(-1)^{j-1} & i+j = m,\ j \leq m/2 \\ \sigma_0(-1)^{m-j} & i+j = m,\ j > m/2 \end{cases} \tag{10}$$

Theorem ([3])

The first order PDE system is stable for all wavenumbers k and all $\tau > 0$ if and only if P is given by (10).

Convergence

$$\mathcal{F}_n = \left\{ v(x) = \sum_{j=1}^{n} \hat{v}_j e^{ik_j x} : \hat{v}, k_j \in \mathbb{R} \right\} \qquad n < \infty. \tag{11}$$

Theorem

Consider the one-dimensional Cauchy problem for (6) with initial data $u(x, t = 0) \in \mathcal{F}$. Let q denote the solution of the hyperbolized system, and let T be given such that $0 \leq T < \infty$. Then

$$\|q_0(x, T) - u(x, T)\|_\infty = \mathcal{O}(\tau). \tag{12}$$

More general PDEs

$$u_t + \sum_{j=0}^{m-1} \alpha_j \partial_x^j u + \sigma_0 \partial_x^m u = 0$$

$\Downarrow$ Hyperbolization

$$\partial_t q_0 + \sum_{j=1}^{m} \alpha_j \partial_x^j q_{j-1} = -\alpha_0 q_0$$

$$\tau \partial_t q_j = \sigma_0 (-1)^j (q_{m-j} - \partial_x q_{m-j-1}) \qquad \text{for } j = 1, 2, \ldots, \left\lceil \frac{m}{2} \right\rceil$$

$$\tau \partial_t q_j = \sigma_0 (-1)^{m-j-1} (q_{m-j} - \partial_x q_{m-j-1}) \quad \text{for } j = \left\lceil \frac{m}{2} \right\rceil + 1, \ldots, m-1$$

More general PDEs

- Identify the highest-order spatial derivative.
- Introduce auxiliary variables for successive derivatives.
- The corresponding linearized model suggests a general strategy for hyperbolizing evolution equations.
- Only the equation for the original variable changes; the auxiliary equations follow a standard form.

Example: the Camassa-Holm (CH) Equation

$$\partial_t u - \partial_t \partial_x^2 u + 3u\partial_x u - 2\partial_x u \partial_x^2 u - u\partial_x^3 u = 0,$$

$$\Downarrow \text{ Hyperbolization}$$

$$\begin{aligned} \partial_t q_0 + 3q_0\partial_x q_0 - 2q_2\partial_x q_0 - q_0\partial_x q_2 - \tau^{-1}(\partial_x q_0 - q_1) &= 0 \\ \tau\partial_t q_1 + (\partial_x q_1 - q_2) &= 0 \\ \tau\partial_t q_2 - (\partial_x q_0 - q_1) &= 0. \end{aligned}$$

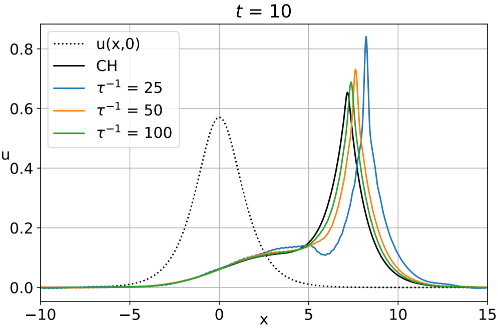

Figure: Comparison of solution of the CH equation and CHH.

Example: the Kuramoto–Sivashinsky (KS) equation

$$\partial_t u + \partial_x^2 u + \partial_x^4 u + u\partial_x u = 0 \Rightarrow \begin{aligned} \partial_t q_0 + \partial_x q_1 + \partial_x q_3 + q_0 \partial_x q_0 &= 0 \\ \tau \partial_t q_1 - (\partial_x q_2 - q_3) &= 0 \\ \tau \partial_t q_2 - (\partial_x q_1 - q_2) &= 0 \\ \tau \partial_t q_3 + (\partial_x q_0 - q_1) &= 0. \end{aligned}$$

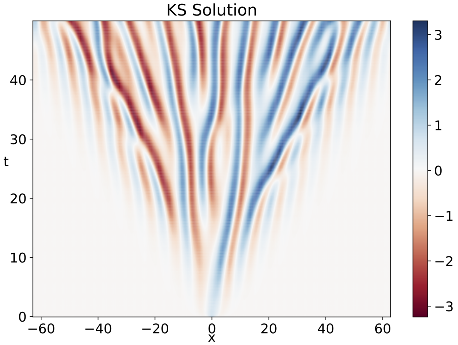

Figure: Solution of the KS equation up to $t = 50$.

Example: the Kuramoto–Sivashinsky (KS) equation

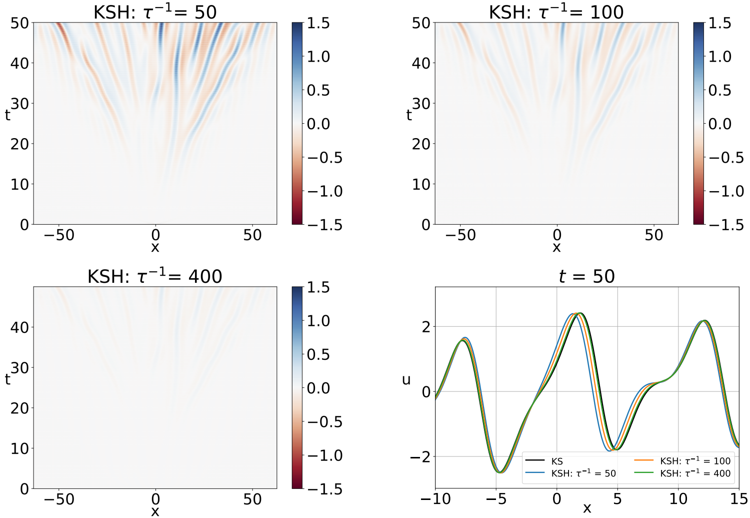

Figure: Pointwise error and solution comparison of KSH and KS for a Gaussian initial condition with three values of relaxation parameter.

Questions?

1. We have removed the "high-order derivative" stiffness, but reintroduced stiffness through τ. Do we win or lose with this exchange?
2. Can we preserve other underlying structure, such as conserved quantities of the original system?
3. What are suitable numerical methods to solve hyperbolized systems?

- Details study of KdV and NLS equations

Hyperbolized KdV

$$\partial_t \eta + \eta \partial_x \eta + \partial_x^3 \eta = 0 \tag{13}$$

A hyperbolic approximation of KdV (KdVH) [2]:

$$\partial_t u + u \partial_x u + \partial_x w = 0 \ , \tag{14a}$$
$$\tau \partial_t v = (\partial_x v - w) \ , \tag{14b}$$
$$\tau \partial_t w = -(\partial_x u - v) \ . \tag{14c}$$

Here $\tau > 0$ is the relaxation parameter.

Traveling waves

- The KdV soliton solutions:

$$\eta(x,t) = 3c\,\mathrm{sech}^2\left(\frac{\sqrt{9c}(x-ct)}{6}\right). \tag{15}$$

- KdVH traveling wave solutions ansatz:

$$u = \tilde{u}(x-ct) \qquad v = \tilde{v}(x-ct) \qquad w = \tilde{w}(x-ct) \tag{16}$$

- Inserting the ansatz into KdVH system yields ODE system:

$$-c\tilde{u}' + \tilde{w}' + \tilde{u}\tilde{u}' = 0 \tag{17a}$$
$$-c\tau\tilde{v}' = \tilde{v}' - \tilde{w} \tag{17b}$$
$$-c\tau\tilde{w}' = -\tilde{u}' + \tilde{v}. \tag{17c}$$

- Manipulate the equation to obtain:

$$\tilde{u}' = \frac{1}{1 + c\tau(\tilde{u} - c)}\tilde{v} \tag{18a}$$
$$\tilde{v}' = \frac{1}{1 + c\tau}(c - \tilde{u}/2)\tilde{u}. \tag{18b}$$

Traveling waves

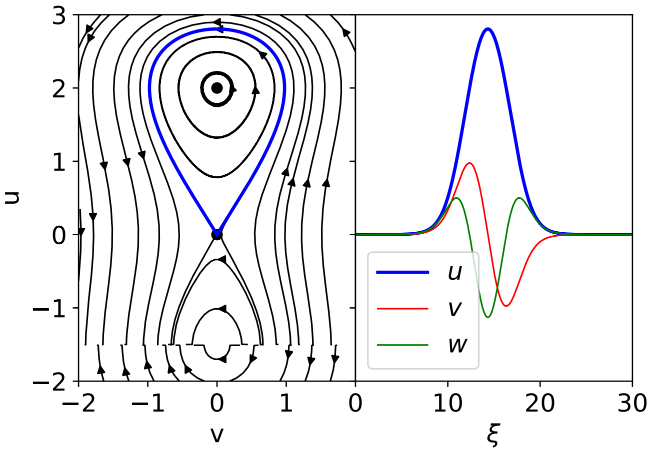

Figure: Phase portrait of the KdVH traveling wave system with $c = 1$ and $\tau = 2/5$. The blue homoclinic orbit connects the saddle point $(0, 0)$, representing a solitary wave of the KdVH system.

Solitary waves: KdV vs. KdVH

- KdV and KdVH solitons have similar shapes.
- KdV solitons can have any positive speed.
- KdVH solitons are limited to speeds with $c^2 < \tau^{-1}$.

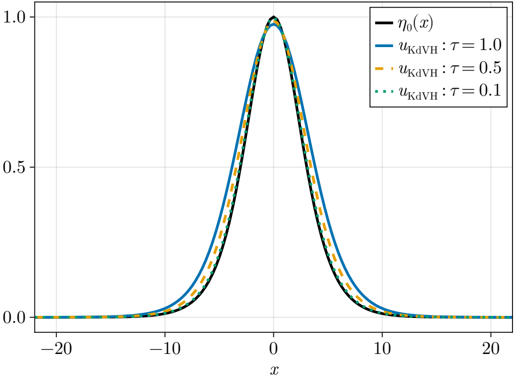

Other traveling waves

$$v_t + cv_x = 0$$
$$w_t + cw_x = 0.$$
$$\Downarrow$$
$$u_t + uu_x + (1+\alpha)u_{xxx} + \alpha(1+\alpha)(u_{xxt} + 3u_x u_{xx} + uu_{xxx}) = 0.$$

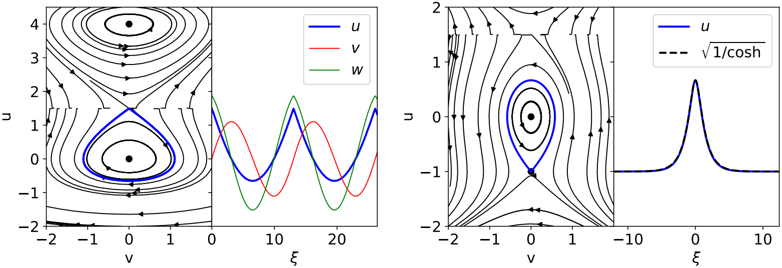

Figure: Traveling wave solutions of KdVH - Left: a right-going peaked periodic wave with speed exceeding the soliton limit. Right: a left-going solitary wave closely resembling $(5/3)\sqrt{\text{sech}(5x/3)} - 1$, shown for comparison.

Efficient space and time discretization of KdVH

$$P^0 : \left\{ \partial_t \eta + \eta \partial_x \eta + \partial_x^3 \eta = 0 \right. \qquad P^\tau : \begin{cases} \partial_t u + u \partial_x u + \partial_x w = 0 \\ \tau \partial_t v = (\partial_x v - w) \\ \tau \partial_t w = -(\partial_x u - v) \end{cases}$$

$$\int \frac{1}{2} \eta^2 \, dx \qquad \int \left(\frac{u^2}{2} + \tau \frac{v^2}{2} + \tau \frac{w^2}{2} \right) dx$$

Goal: To design fully discrete asymptotic preserving and energy conserving numerical methods

- Structure-preserving spatial discretizations based on summation-by-parts operators
- Asymptotic-Preserving time discretization via ImEx methods
- Energy conservation via RK relaxation

Energy-conserving spatial semidiscretization

$$P^0 : \left\{ \partial_t \eta + \eta \partial_x \eta + \partial_x^3 \eta = 0 \right. \quad \Rightarrow \quad \partial_t \boldsymbol{\eta} + \frac{1}{3}\left(D\boldsymbol{\eta}^2 + \boldsymbol{\eta} D\boldsymbol{\eta} \right) + D_+ D D_- \boldsymbol{\eta} = \mathbf{0}$$

$$P^\tau : \begin{cases} \partial_t u + u \partial_x u + \partial_x w = 0 \\ \tau \partial_t v = (\partial_x v - w) \\ \tau \partial_t w = -(\partial_x u - v) \end{cases} \quad \Rightarrow \quad \begin{aligned} \partial_t \boldsymbol{u} + \frac{1}{3}\left(D\boldsymbol{u}^2 + \boldsymbol{u} D\boldsymbol{u} \right) + D_+ \boldsymbol{w} = \mathbf{0}, \\ \partial_t \boldsymbol{v} + \frac{1}{\tau}\left(-D\boldsymbol{v} + \boldsymbol{w} \right) = \mathbf{0}, \\ \partial_t \boldsymbol{w} + \frac{1}{\tau}\left(D_- \boldsymbol{u} - \boldsymbol{v} \right) = \mathbf{0}\ , \end{aligned}$$

where $D_-,\ D,\ D_+$ are periodic first-derivative finite difference SBP operators.

AP and AA time discretization

$$P^0 : \eta_t = \underbrace{-\eta\eta_x}_{=f(\eta)} \underbrace{-\eta_{xxx}}_{=g(\eta)} \tag{19}$$

$$P^\tau : \underbrace{\begin{pmatrix} u \\ v \\ w \end{pmatrix}_t}_{=q_t} = \underbrace{\begin{pmatrix} -uu_x \\ 0 \\ 0 \end{pmatrix}}_{=f(q)} + \underbrace{\begin{pmatrix} -w_x \\ \frac{1}{\tau}(v_x - w) \\ \frac{1}{\tau}(-u_x + v) \end{pmatrix}}_{=g(q)} . \tag{20}$$

- A scheme is AP if it reduces to a consistent discretization of the original problem as $\tau \to 0$.
- For this problem, most ImEx schemes are AP for u, but only some are AP for v and w.
- A numerical scheme P_h^τ is AA if, in the limit $\tau \to 0$, it retains its temporal order of accuracy for the limit scheme P_h^0.

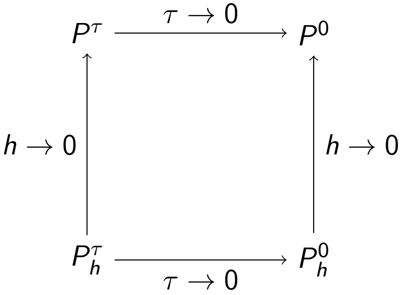

Asymptotic-preserving time discretization

Theorem

An ImEx-RK method of type I applied to the splitting (20) of the hyperbolic approximation of the KdV equation is always AP for the u-component. For such a method, in the relaxation limit $\tau \to 0$, we have

$$u^{n+1} - \eta(t_{n+1}) = \mathcal{O}(\Delta t^p) \; , \tag{21}$$

where p is the order of the ImEx-RK method. Furthermore, if the method is assumed to be globally stiffly accurate, it is also AP for the auxiliary components v and w. In the relaxation limit $\tau \to 0$, we have

$$v^{n+1} - \eta_x(t_{n+1}) = \mathcal{O}(\Delta t^p) \quad \text{and} \quad w^{n+1} - \eta_{xx}(t_{n+1}) = \mathcal{O}(\Delta t^p) \; . \tag{22}$$

Energy conservation via RK relaxation

Consider

$$q_t = f(q) + g(q), \quad q(0) = q^0,$$

with the energy invariant denoted by $I(q)$.

- Using an ImEx method, we require $I(q^{n+1}) = I(q^n) = I(q^0)$ at the discrete level.
- Modify the solution update using a scalar relaxation parameter

  $$q(t_n + \gamma_n \Delta t) \approx q^{n+1}_{\gamma_n} = q^n + \gamma_n \Delta t \left(q^{n+1} - q^n\right),$$

  and choose γ_n to satisfy the nonlinear scalar equation

  $$I(q^{n+1}_{\gamma_n}) = I(q^n).$$

- Under certain mild conditions, $\gamma_n = 1 + \mathcal{O}(\Delta t^{p-1})$.

Numerical tests of asymptotic preservation

Table: Asymptotic errors and estimated orders of convergence (EOC) for the SSP2-ImEx(2,2,2) method.

τ	$\|\|\boldsymbol{u}-\boldsymbol{\eta}\|\|_2$	EOC $\boldsymbol{u}$	$\|\|\boldsymbol{v}-D_{-}\boldsymbol{\eta}\|\|_2$	EOC $\boldsymbol{v}$	$\|\|\boldsymbol{w}-DD_{-}\boldsymbol{\eta}\|\|_2$	EOC $\boldsymbol{w}$
1.00e-01	3.77e+00		3.13e+00		3.61e+00	
1.00e-03	5.35e-02	0.92	4.47e-02	0.92	5.55e-02	0.91
1.00e-05	5.37e-04	1.00	8.96e-03	0.35	1.63e-02	0.27
1.00e-07	5.37e-06	1.00	9.51e-03	-0.01	1.69e-02	-0.01
1.00e-09	5.39e-08	1.00	9.52e-03	-0.00	1.69e-02	-0.00

Table: Asymptotic errors and estimated orders of convergence (EOC) for the ARS(4,4,3) method.

τ	$\|\|\boldsymbol{u}-\boldsymbol{\eta}\|\|_2$	EOC $\boldsymbol{u}$	$\|\|\boldsymbol{v}-D_{-}\boldsymbol{\eta}\|\|_2$	EOC $\boldsymbol{v}$	$\|\|\boldsymbol{w}-DD_{-}\boldsymbol{\eta}\|\|_2$	EOC $\boldsymbol{w}$
1.00e-01	3.76e+00		3.13e+00		3.60e+00	
1.00e-03	5.34e-02	0.92	4.88e-02	0.90	6.31e-02	0.88
1.00e-05	5.36e-04	1.00	4.89e-04	1.00	6.31e-04	1.00
1.00e-07	5.36e-06	1.00	4.89e-06	1.00	6.31e-06	1.00
1.00e-09	5.38e-08	1.00	5.23e-08	0.99	6.50e-08	0.99

Numerical tests of asymptotic accuracy

Definition (Asymptotic accuracy (AA))

A numerical scheme P_h^τ is AA if, in the limit $\tau \to 0$, it retains its temporal order of accuracy for the limit scheme P_h^0.

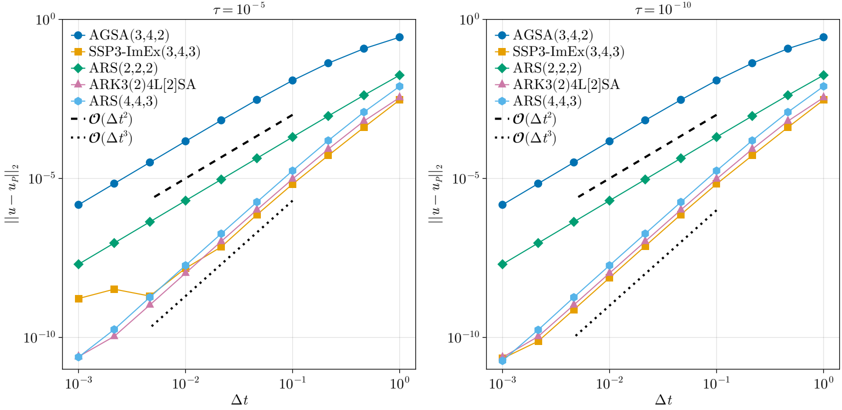

Figure: Error convergence for u component. The reference solution u_P is computed using a Petviashvili-type method.

Numerical tests of asymptotic accuracy

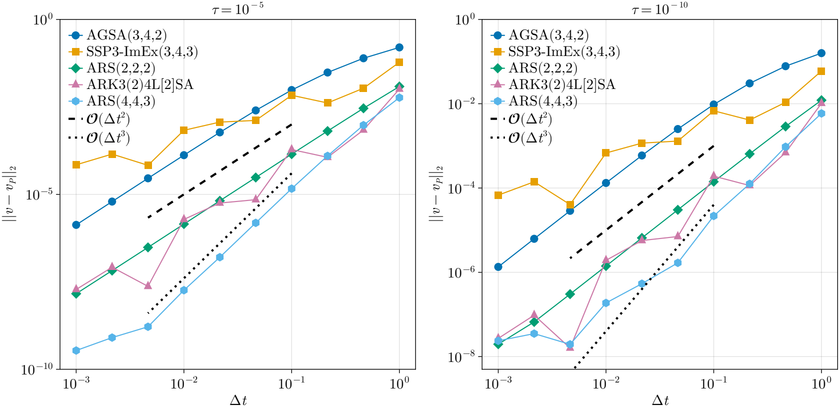

Figure: Error convergence for v component. The reference solution v_P is computed using a Petviashvili-type method.

Numerical tests of asymptotic accuracy

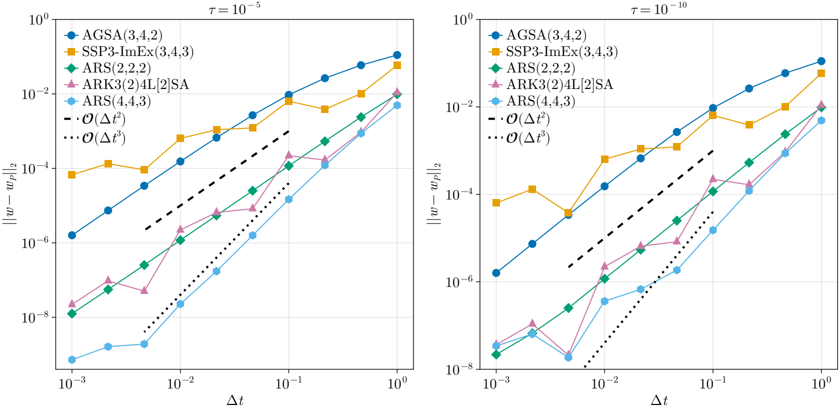

Figure: Error convergence for w component. The reference solution w_P is computed using a Petviashvili-type method.

Numerical tests of energy conservation

- Energy conservation can be enforced via relaxation in time
- At early times, hyperbolization error dominates
- At late times, truncation error dominates (greatly reduced by temporal relaxation)

Error growth profile: $\tau = 10^{-3}$

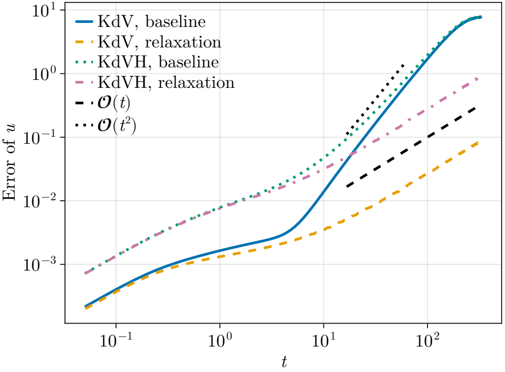

Hyperbolized NLS: motivation

The nonlinear Schrödinger (NLS) equation

$$iu_t + u_{xx} + \kappa|u|^2 u = 0, \quad -\infty < x < \infty, \quad t > 0. \qquad (23)$$

- Dhaouadi et al. studied a hyperbolization of the defocusing NLS ($\kappa < 0$) equation written in hydrodynamic form using Madelung transform.
- The system of two equations in hydrodynamic form can be seen as the Euler–Lagrange equations for a Lagrangian.
- Using an extended Lagrangian they form a hyperbolic approximation system of five equations that admits a conserved energy.

Hyperbolized NLS: our approach

The hyperbolized NLS (NLSH) [1]

$$i\partial_t q_0 + \partial_x q_1 = -\kappa |q_0|^2 q_0 \ , \tag{24a}$$

$$i\tau\partial_t q_1 = \partial_x q_0 - q_1 \ , \tag{24b}$$

where $q_0 \approx u$ and $q_1 \approx \partial_x q_0$.

- Strictly hyperbolic system of 2 equations
- Applicable in both focusing ($\kappa < 0$) and defocusing ($\kappa > 0$) regimes
- Analogous Hamiltonian structure
- Preserves analogues of multiple conserved quantities

Hamiltonian structure

$$\begin{cases} iu_t + u_{xx} + \kappa|u|^2 u & = 0 \end{cases} \qquad \begin{cases} i\partial_t q_0 + \partial_x q_1 = -\kappa|q_0|^2 q_0 \ , \\ i\tau\partial_t q_1 = \partial_x q_0 - q_1 \ . \end{cases}$$

- Hamiltonian:

$$H = \int_{\mathbb{R}} \left(|u_x|^2 - \frac{\kappa}{2}|u|^4 \right) dx$$

- Modified Hamiltonian:

$$\bar{H} = \int_{\mathbb{R}} \left(q_1^* \partial_x q_0 + q_1 \partial_x q_0^* - |q_1|^2 - \frac{\kappa}{2}|q_0|^4 \right) dx$$

- Mass:

$$I_1(t) = -\int_{\mathbb{R}} |u|^2 \, dx$$

- Modified Mass:

$$\bar{I}_1(t) = -\int_{\mathbb{R}} \left(|q_0|^2 + \tau|q_1|^2 \right) dx$$

- Momentum:

$$I_2(t) = -i \int_{\mathbb{R}} u^* u_x \, dx$$

- Modified Momentum:

$$\bar{I}_2(t) = -i \int_{\mathbb{R}} \left(q_0^* \partial_x q_0 + \tau q_1^* \partial_x q_1 \right) dx$$

Standing waves: focusing case

- Standing wave of NLS:

$u^+(x) = \sqrt{2}\sigma \operatorname{sech}(\sqrt{\mu}x \pm K_1)$ with $\mu, \kappa > 0$ and $\sigma = \sqrt{\frac{\mu}{\kappa}}$.

- Standing wave of NLSH:

$q_0^+(x) := \sqrt{2}\sigma \operatorname{sech}(\sqrt{\mu(1-\mu\tau)}x \pm K_1)$

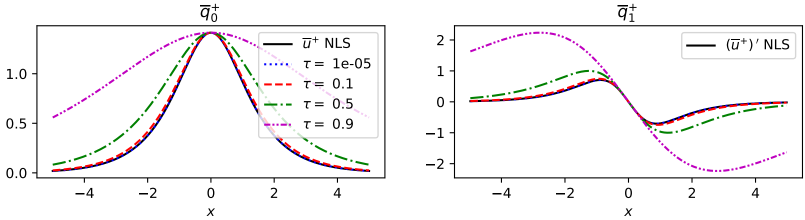

Figure: Standing wave solutions to the NLSH system and the NLS equation with $\kappa = \mu = 1$, $K_1 = 0$, and different values of τ

Standing fronts: defocusing case

- Standing front of NLS:

$u^-(x) = \sigma \tanh(\pm\sigma\sqrt{-\kappa/2}x \pm K_0)$ with $\mu, \kappa < 0$ and $\sigma = \sqrt{\frac{\mu}{\kappa}}$.

- Standing front of NLSH:

$$q_0^-(x) = \sigma \tanh\left(\pm\sigma\sqrt{\frac{\kappa(\mu\tau-1)}{2}}x \pm K_0\right)$$

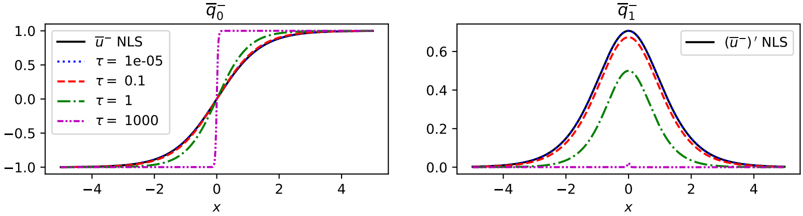

Figure: Standing front solutions to the NLSH system and the NLS equation with $\kappa = \mu = -1$, $K_0 = 0$, and different values of τ

Efficient space and time discretization of NLSH

$$P^0 : \begin{cases} iu_t + u_{xx} + \kappa |u|^2 u = 0 \end{cases} \qquad P^\tau : \begin{cases} i\partial_t q_0 + \partial_x q_1 = -\kappa |q_0|^2 q_0 \,, \\ i\tau \partial_t q_1 = \partial_x q_0 - q_1 \,. \end{cases}$$

$$\int_{\mathbb{R}} |u|^2 \, dx \qquad \int_{\mathbb{R}} \left(|q_0|^2 + \tau |q_1|^2 \right) dx$$

Goal: To design fully discrete asymptotic preserving and mass-conserving numerical methods

- Structure-preserving spatial discretizations based on the Fourier spectral differentiation matrix
- Asymptotic-Preserving time discretization via ImEx methods
- Energy conservation via RK relaxation

Mass-conserving spatial semidiscretization

- Q_0, Q_1 with $(Q_0)_j(t) \approx q_0(x_j, t)$ and $(Q_1)_j(t) \approx q_1(x_j, t)$.
- Semi-discretization:

$$\partial_t Q_0 = iDQ_1 + i\kappa L Q_0 \tag{25a}$$

$$\tau \partial_t Q_1 = iQ_1 - iDQ_0, \tag{25b}$$

where L is the diagonal matrix with entries $\ell_{jj} = |(Q_0)_j|^2$ and D is a matrix that approximates the first derivative operator.

Theorem

If D is skew-hermitian, then solutions of (25) are mass conservative:

$$\frac{d}{dt}\left(\|Q_0\|^2 + \tau \|Q_1\|^2\right) = 0. \tag{26}$$

AP and mass-conserving time discretization

$$P^0 : u_t = \underbrace{i\kappa |u|^2 u}_{=f(u)} + \underbrace{iu_{xx}}_{=g(u)} \tag{27}$$

$$P^\tau : \underbrace{\begin{pmatrix} q_0 \\ q_1 \end{pmatrix}_t}_{=Q_t} = \underbrace{\begin{pmatrix} i\kappa |q_0|^2 q_0 \\ 0 \end{pmatrix}}_{=f(Q)} + \underbrace{\begin{pmatrix} i\partial_x q_1 \\ -i\tau^{-1}(\partial_x q_0 - q_1) \end{pmatrix}}_{=g(Q)}. \tag{28}$$

Theorem

A GSA ImEx-RK method of type II, applied to the splitting (28) of the NLSH system, together with the well-prepared initial data, is AP for both q_0 and q_1. Furthermore, in the relaxation limit $\tau \to 0$, the following error estimates apply to all components:

$$q_0^{n+1} - u(t_{n+1}) = \mathcal{O}(\Delta t^p), \quad q_1^{n+1} - u_x(t_{n+1}) = \mathcal{O}(\Delta t^p),$$

where p is the order of the ImEx-RK method.

- Fully-discrete conservation can be enforced via relaxation in time.

Numerical tests of asymptotic preservation

Table: Errors and EOC for the 2-soliton problem with SSP3-IMEX(3,4,3).

τ	$\|u - q_0\|_2$	EOC q_0	$\|Du - q_1\|_2$	EOC q_1
0.01	4.411e-01		4.966e-01	
0.0001	7.697e-03	0.879	1.301e-02	0.791
1e-06	7.744e-05	0.999	1.347e-04	0.992
1e-08	7.744e-07	1.0	2.081e-04	-0.095
1e-10	7.744e-09	1.0	2.092e-04	-0.001

Table: Errors and EOC for the 2-soliton problem with ARS(4,4,3).

τ	$\|u - q_0\|_2$	EOC q_0	$\|Du - q_1\|_2$	EOC q_1
0.01	4.411e-01		4.966e-01	
0.0001	7.697e-03	0.879	1.301e-02	0.791
1e-06	7.744e-05	0.999	1.317e-04	0.997
1e-08	7.744e-07	1.0	1.318e-06	1.0
1e-10	7.744e-09	1.0	1.317e-08	1.0

Focusing NLS test case: multi-soliton bound states

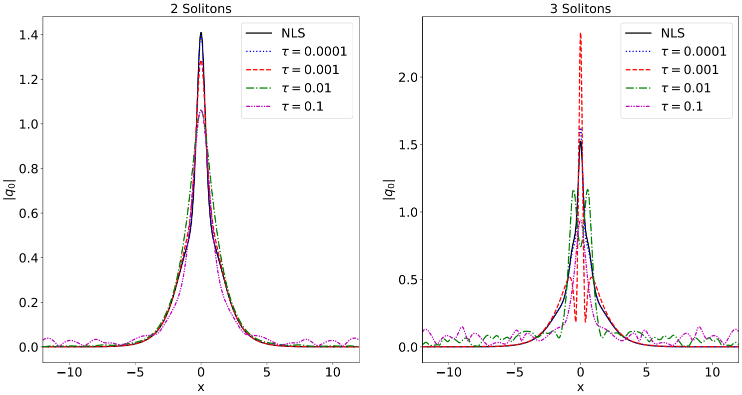

Figure: Bound state soliton solutions for 2 (left) and 3 (right) solitons. As $\tau \to 0$ the NLSH solution converges to NLS solution.

A defocusing NLS test case: smoothed Riemann problem

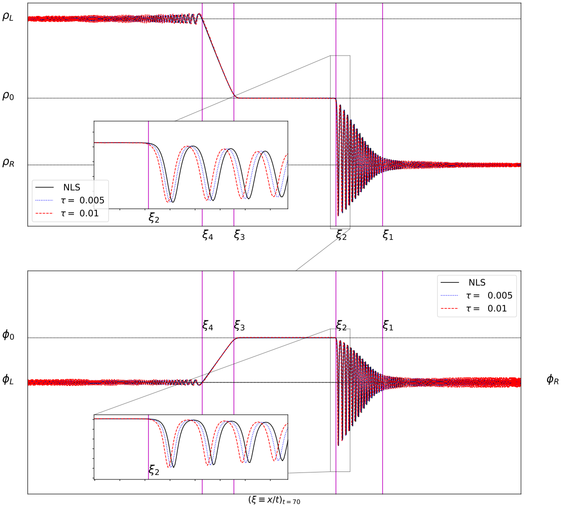

Figure: Solution of defocusing NLS at $t = 70$ with initial smoothed step function.

Some Current and Future Work

- Efficient numerical discretizations for hyperbolic approximations of BBM and Camassa–Holm equations
- Application of exponential time integrators
- Tsunami modeling using a combination of shallow water and hyperbolized Boussinesq-type models
- Hyperbolic approximation of the NLS equation in higher dimensions

Conclusions

- Many high-order PDEs can be approximated by hyperbolic PDEs
- Hyperbolization is unique and convergent for a special class of linear PDEs.
- A general approach provides stable hyperbolic approximations for evolution PDEs.
- Applicable to many nonlinear PDEs, with strong supporting numerical evidence.
- This might provide interesting new applications for existing numerical methods.

References

[1] Abhijit Biswas et al. “A Hyperbolic Approximation of the Nonlinear Schrödinger Equation”. In: *arXiv preprint arXiv:2505.21424* (2025).

[2] Abhijit Biswas et al. “Traveling-wave solutions and structure-preserving numerical methods for a hyperbolic approximation of the Korteweg-de Vries equation”. In: *Journal of Scientific Computing* (2025).

[3] David I Ketcheson and Abhijit Biswas. “Approximation of arbitrarily high-order PDEs by first-order hyperbolic relaxation”. In: *Nonlinearity* 38.5 (2025), p. 055002.